https://dx.doi.org/10.22161/ijaers.4.4.41 *ISSN: 2349-6495(P) | 2456-1908(O)*

Electro-synthesized Conjugated Salen Polymer-Glassy Carbon as Hydrochromic Reflective Filter for Humidity Detection: Introduction of Humidity Optical Sensor

Mohammad Mahdi Doroodmand, Sina Owji

Department of Chemistry, College of Sciences, Shiraz University, Shiraz 71454, Iran.
*Corresponding Author: (M. M. Doroodmand) doroodmand@shirazu.ac.ir, Tel: +098-711-6137363, Fax: +098-711-2286008.

***Abstract*—** *A novel humidity optical sensor was fabricated based on adsorption of water vapor via the hydrochromic reflective filtration behavior of conjugated Salen polymer, immobilized on the surface of a glassy carbon (GC) electrode by cyclic voltammetry (CV). This process was attributed to the hydrophilic behavior of the electro-synthesized conjugated Salen-based polymer when contacting with water vapors especially during coordination with K^+ through the electro-synthesis process. Optical image of the hydrochromic reflective filter was considered as appropriate detection system for relative humidity (RH) sensing purpose. The mechanism of the change in the color intensity was evaluated via optical filtration of a white laser diode as polychromatic optical source via filtration by the conjugated polymer during its reflection from a smooth surface such as GC. The GC electrode therefore acted as both i) the working electrode during the electrochemical synthesis by CV, and ii) light reflector (mirror) during the light radiation. In this study the electrochemical and optical properties of the GC was compared to a graphite or metal electrode. Parameters such as linearity, rise/fall time, sensitivity, and selectivity of each the fabricated humidity optical sensor were evaluated. Also, dependency of humidity sensor to temperature was investigated. The intensity of the blue component was linearly increased over a wide range of RH between 5 - 80%. The fabricated optical sensor had improved detection limit (0.17% RH), standard saturated limit (>80% RH), accepted relative standard deviation (RSD= 3.6%, n=3), short rise time (~9.5 s compared to the commercial RH sensor), good linearity (R=0.9971) and maximum~7.5 % RH hysteresis. Effects of interferences such as H_2, CO, CO_2, NOx, He, and volatile organic compounds (VOCs) were also considered. Results showed no noticeable interfering effects. This sensor was applicable for selective and reliable detection of %RH in different environmental samples without having any significant interferences.*

***Keywords*— Electro-synthesis; Conjugated Salen polymer; Hydrochromic reflective filter; Humidity sensor.**

I. INTRODUCTION

Humidity quantity is considered as one of the most important scientific topics in different branches of fields such as food industry, biology, chemistry, medicine, drug delivery, agriculture, automobiles, etc. According to the literature, humidity detection methodology, relative humidity (RH), Dew/Frost point (D/F point) and "parts per million" (ppm) are the most common techniques [1]. RH is defined as the fractional pressure of water vapors in air that implies the saturated vapor pressure. This term is powerfully attributed to the moisture content (absolute humidity), temperature and pressure. The RH value is often adopted while the rate of water evaporation is significant. Dew point is also attributed to the temperature upon which water vapors are concentrated to the water. This term designates the quantity of RH. The higher the relative humidity, the smaller difference is existed between the dew point and the air temperature. The phrase "ppm", as a new absolute measurement has widespread functions in industry, particularly for the trace moisture detection [2]. Among these units, RH that studied in this work, is commonly used with medium or ambient levels of the humidity. Consequently, powerful, economical, consistent, receptive and specific humidity sensors is very focal subject [3].

During the last decades, different sensing technologies based on change in the intensity of electromagnetic waves [4], or via recording the changes in the electrical properties such as impedance [5], capacity [6], or the frequency of

https://dx.doi.org/10.22161/ijaers.4.4.41 *ISSN: 2349-6495(P) | 2456-1908(O)*

surface acoustic waves (SAWs) [7], inter-digitated circuit[8], electronic devices such as field effect transistors (FETs) [9-11], quartz crystal microbalance [12-15] and optical detection system [16], have been investigated for humidity detection and determination. However between these ranges of sensing methods, optical sensing has been selected in this study, because of its significant advantages such as improved detection system, fast response time, high sensitivity and its wide linear response [16].

In the fabrication of the optical sensing devices, often conductive polymers are adopted [6]. Briefly conductive polymers as metal conductive materials or semiconductors are selected as organic polymers that conduct electricity. These conductive polymers are fabricated using different chemical or electrochemical methods [3].

Among the introduced synthetic methods for the generation of conductive polymers, electros-synthesis is considered as selective techniques that often lead to have polymer with defined morphology and acceptable purity. Along with the introduced conductive polymers such as polyphenylenes, polypyrenes, polypyrroles, etc. [17], Salen-based polymer is considered as polymer with partial conductivity [18]. Based on the literate, a new electroactive and sometimes conducting polymers based on metal-Salen containing units has been prepared by electro-oxidation of mononuclear transition metals ion complexes and found to exhibit the electrochemical features of the metal system, associated with the reversible oxidation of the ligand [18]. However in spite of the great developments of the optical-based sensors, but to the best of knowledge no reliable humidity-based optical sensors have been introduced. This problem is probably attributed to some major challenges such as limited sensitivity of conductive polymer during interaction with water molecules, high cost of the general optical sensors, etc. To solve these problems hereby in this work, a simple method is introduced for fabrication of humidity sensor using electro-synthetic conductive polymer using Salen molecule.

II. EXPERIMENTAL

2.1. Reagents and Materials

All the chemical reagents were from their analytical grades. Inorganic salts such as KCl, NaCl and LiCl with >99% purity percentage were all from Merck Company. Analytical grades of non-aqueous solvents such as CH_3OH (purity: 99.9 %, GMW= 32.04 g mol^{-1}), C_2H_5OH (purity: 99.5 %, GMW= 46.07 g mol^{-1}), C_3H_8OH (purity: 99.5 %, GMW= 60.1 g mol^{-1}), DMF (purity: 99.8 %, GMW= 73.09 g mol^{-1}), DMSO (purity: 99.9 %, GMW= 78.13 g mol^{-1}), and acetone (purity: 99.5 %, GMW= 58.08g mol^{-1}) were purchased from Merck company. Deionized water (conductivity: 1 micro-Zimens) was also adopted as water solvent. To synthesize the Salen monomer, salicyle aldehyde (Analytical grade, purity: >99 %, GMW= 122.12 g mol^{-1}) and ethylene diamine (Analytical grade, purity: >99 %, GMW= 60.10 g mol^{-1}) were from the Merck company. Also potassium salts of $Fe(CN)_6^{3-/4-}$were from Merck company. The pH of the electrolyte was controlled using HCl (purity: 32.0 %, w/w, Merck), and NaOH (purity: >99 %, Merck).

2.2. Apparatus

The three-electrode system included GC as working electrode, Ag/AgCl (sat'd Cl^-) as reference electrode and a Pt rode as counter electrode. The cyclic voltammetry (CV) was performed with a Potentiostate–Galvanostate, μAutolab type III. All the experiments were conducted at 25±2 °C. Also a fluorescence optical microscopy (model: CETI-Magnum T) was adopted for imaging the synthesized thin film polymer. Photographic images from the electrode surfaec were captured using a digital Camera (model: AGPtek, magnifying ratio: X 800). The morphology of the synthesized polymer was also evaluated using scanning electron microscopy (SEM, KYKY-EM3200). A chamber with 1500 mL volume was made of glass plates that assembled all the components of Humidity sensor system. This system included a reference humidity sensor (Model: Lutron GCH-2018), a glassy carbon (GC) electrode deposited polymer as probe, a thermometer, a tiny fan, an infra-red (IR) source (model: HG-IR1XYJ-F-1W), air input/output ports, and a camera for capturing the surface of the probe. All these components were assembled to a fixed position on the glassy chamber. The chamber was covered by a black coverage to prevent exposing the light in chamber. Required light was supplied for the imaging process by the camera.

2.3. Synthesis of Salen and Salen-Based Polymer

To synthesize the Salen, 200 mL dried ethanol was added to 0.10 mole (GMW= 122.12 g $mole^{-1}$, V=10.6 mL) of salicylealdehyde and stirred at room temperature according the procedure reported in Ref. [19]. After that 0.05 mole (V= 3.3 mL) ethylenediamine was slowly added. After about several seconds, a yellow precipitation was observed. To complete the reaction, the solution was stirred for ~30 min at room temperature. Then the temperature of the suspension was set to around zero temperature using an ice bath. The precipitation was then separated via filtration

https://dx.doi.org/10.22161/ijaers.4.4.41 *ISSN: 2349-6495(P) | 2456-1908(O)*

through a paper filter (mesh: 300). The precipitation was then washed using 200 mL cooled ethanol-water (50% V/V) for three times. Finally the precipitation was dried at 50 ^{o}C using an oven.

To electro-synthesize the Salen-based polymer, the potential window was set from -1.0 to +2.25 V (vs. Ag/AgCl) at scan rate of 100 mV s^{-1}on the surface of the GC as working electrode. This process led to have anodic polymerization process during observation of an anodic peak current at potential ~+0.70 V (vs. Ag/AgCl) during formation of complex between polymeric Salen and K^{+}. Then during sweeping the potential to a negative potential such as (-1.0 V, vs. Ag/AgCl), three independent anodic peaks were observed at potential of ~ +0.5, +1.25 and +1.75 V (vs. Ag/AgCl), respectively during formation of conjugated Salen-based polymer on the surface of the GC electrode. Then the surface of the electrode was washed with distillated water and dried in air atmosphere. The modified electrode was finally adopted for evaluation of its application for the humidity sensing purpose.

2.4. Apparatus

Fig. 1 shows the schematic of the designed apparatus for humidity detection and measurement. To evaluate the capability of the electro-synthesized Salen-based polymer on the surface of the carbon electrode, a glass cubic cell with volume to around 1500 mL (dimension: 10×10×15 cm) was fabricated. Then the modified GC electrode was introduced from one side of the cell. Also from the opposite, side a white light LED, as well as a digital camera (model: AGPtek, magnifying ratio: X 800) were positioned with angle between 10-20^{o} versus the GC carbon electrode. Also to remove the hysteresis of the GC electrode from any adsorption and diffusion of humidity, an IR light source was positioned next to the GC electrode to eliminate the memory effect. In addition, N_2 gas (purity: 99.995) was selected as solvent during making the humidity standard solutions. To introduce the humidity to the cell, an ultrasonic source was assembled in a glassy box for introduction of transmitted humidified air to the cell. The standard humidity solutions were also standardized using a Ref. humidity sensor (model: Lutron GCH-2018). To prevent arrival of the stray light, the cell was positioned in a dark room via painting the external surface of the glass cell with black color.

2.5. Procedure

Before starting the humidity detection process, the memory effect of the sensors was eliminated via radiation of the Salen-based electrode system with the IR light for ~0.5 min. Also the space inside the glass cell was cleaned from any water vapor (humidity) via purging N_2 gas as inert gas solvent for ~ 1 min with flow rate of ~2 L min^{-1}. Then the humidifier (humidity generator) was turned on for essential time to introduce water aerosols to the glass cell by the use of N_2 as both gaseous solvent and carrier gas. The standardization of the standard humidity concentrations was achieved using the humidity Ref. sensor. After cooling the Salen-based GC support to the room temperature, the white light (optical source) was turned on and the optical changes in the color was imaged during filtration by the Salen-based GC support along 5 s time interval at ~ 25 ^{o}C temperature and ambient pressure as standard temperature and pressure (STP). After saving the optical images in a PC, the images were processed using Photoshop software (version: CC 16.1.2). The schematic of the analysis using the software has been shown in Sc hem. 1. For this purpose combination of the blue or green component of each image was selected as humidity measuring probe.

2.6. Real sample analysis

The reliability of this sensor was evaluated via analyses of different real samples such as the air atmosphere of the urban tunnel, lab air, automobile exhaust air, etc. For this purpose, each sample was accumulated in a plastic balloon (~2 L) using a membrane pump (model: Tornado AC580). After cleaning the glass cell as well as elimination of any probable memory effect from the previous analysis using the procedure reported in the previous section, each sample was introduced to the cell directly with ~1.0 L min^{-1} flow rate for ~ 1 min time interval and the images were processed according to the recommended procedure.

III. RESULTS AND DISCUSSION

Salen is considered as the family of Schiff bases, derived from ethylenediamine and ortho-phenolic aldehydes (N, N'-ethyleneis(salicylideneiminato) Salen). In these polymers to enhance their electrical conductivity as well as to control their polarity, they are often coordinated with metal ion species such as Al, Ce, Co, Cu, Cr, Fe, Ga, Hg, Mn, Mo, Ni, and V [20]. This relationship often lead to have more conductive polymer, which is suitable for various catalytic purposes such as electro-catalyst in the electrochemical processes [21]. In these complexes, the conductivity is majorly attributed to the metal ion species, compared to the Salen monomer or polymer, which possessed small dielectric constant. In another word, the polarity of the Salen-based complex is promoted during coordination with

https://dx.doi.org/10.22161/ijaers.4.4.41 *ISSN: 2349-6495(P) | 2456-1908(O)*

metal species [22]. All of these characteristics have made the current Salen-based sensors to be considered as metal-based sensors.

3.1. Electro-synthesis of Salen polymer, successive cyclic voltammetry

The continuous CV of Salen monomer during the electro-synthesis of Salen (0.04M) at potential ranging between -1.0 - +2.25 V and scan rate of 100 mV s^{-1} has been shown in Fig. 2.A. As shown, observation of a strong peak in the first scan of potential at ~+0.70 V (vs. Ag/AgCl) was related to the anodic electro-synthesis of the Salen polymer. However, during the continuous CV from the second scan, significant decrease was observed in the peak intensity (anodic peak current). As clearly evaluated, the higher the number of cycles, the lower was the anodic peak intensity after the first CV cycle. This phenomenon was related to the non-conductivity of the synthesized Salen polymer. This problem has been considered as serious challenge for fabrication of various electrochemical probes during modification of the working electrode by Salen polymer. However to the best of knowledge from the earliest literature review, all the reports have focused on the use of metal/Salen instead of free Salen monomer [23]. This technique therefore led to have a conductive polymer via evaluation of the redox behavior of coordinated metal ions. But in this study for this first time it has been reported that, continuous CVs lead to have three independent anodic peaks. This observation clearly pointed to the effective role of the proposed procedure for formation of new type of Salen-based polymer using Salen as monomer.

3.2. Effect of solvent

Based on the literature, the electro-synthesis of Salen-based polymer was provided inside organic solvents such as DMF, DMSO, etc. The choice of organic solvent was based on the solubility of metal/Salen complex. In this study from one side, Salen monomer was adopted and from the other side the electrical charge enhanced its solubility inside partially polar solvents such as H_2O, alcohol, acetone, etc. Therefore, in this study it was focused on less toxic and greener solvents. In addition, higher polarity of these solvents simply decreased the ohmic potential of the electrolyte, resulting in the need of less positive electrical potential for the electro-synthesis of the conjugated Salen polymer. Effect of different solvent such as propanol, sulfolane, methanol, dimethyle formamide (DMF), acetone, ethanol, diethylether, 1-butanol, and isobutanol has been evaluated according to the CVs shown in Fig. 2.B. Some solvents such as diethylether, 1-butanol and isobutanol did not produce a single-phase and transparent solution. Therefore acetone was selected as solvent during the electro-synthetic process.

As shown (Fig. 2.B), significant enhancements were observed in the anodic peak currents during using solvents such as CH_3OH, C_2H_5OH and acetone. More sensitive signals were observed when using acetone in comparison with alcohols. Therefore, acetone was selected as appropriate solvent. Based on the results, maximum sensitivity was eva
optimum ratio.

3.3. Effect of pH and ionic strength

Mixture of acetone:water as electrolyte from one side was miscible inside each other and from the other side provided the possibility to control the basicity and the ionic strength of the electrolyte. As explained no Salen-based polymer was generated under the acidic conditions due to the decomposition of the Salen monomer. Therefore, the optimization process was evaluated at different pH values between ~7 to above 13. Fig. 4 shows the CVs during the electro-synthesis using Salen (0.04 M) at 100 mV s^{-1} scan rate at various pH values using different concentrations of KOH and HCl. Based on the results (Fig. 4), the higher the pH values, th

3.4. Kind and concentration of cation

To evaluate the effect of cations during the polymerization of Salen polymer, the effect of various cations such as K^+, Na^+, Li^+, Ca^{2+}, Ba^{2+}, Mg^{2+}, Al^{3+}, etc. were evaluated in detail. Insoluble precipitations were observed during formation of complexes of Salen with Ca^{2+}, Ba^{2+}, Mg^{2+}, Al^{3+}, etc. As cations with two or three capacities were insoluble inside the solvent, therefore it was only focused on the cations with one capacity such as K^+, Na^+ and Li^+. Fig. 5 shows the CVs during the electro-polymerization of polymer using Salen (0.04 M) at scan rate of 100 mVs^{-1} at strong basic condition controlled using the same concentrations of each LiOH, NaOH and KOH under similar conditions. The sequence of sensitivity of the anodic peak currents were as follows: $K^+ > Na^+ > Li^+$. Therefore, the higher the diameter of the cations, the more conductive polymer was synthesized. This effect was further evaluated via image processing the Salen polymer-modified GC electrode at an environment with ~40% humidity.

Based on the images (Fig. 6), the same correction was observed between the color of the polymer with the atomic spectrum during analysis of K^+, Na^+ or Li^+. Whereas no clear color was observed during narrowing the potential window ranging from -1.0 to 2.25 V (vs. Ag/AgCl). This

https://dx.doi.org/10.22161/ijaers.4.4.41 *ISSN: 2349-6495(P) | 2456-1908(O)*

observation from one side pointed to the coordination of cations at the negative potentials and from the other side revealed the hydrophilicity of the synthesized Salen-based polymer. In this study due to the availability of KOH, this reagent was selected for controlling the pH of the electrolyte. This effect was again evidenced via addition of different concentrations of KCl. Further concentrations of K^+ were optimized during addition of different concentrations of KCl between 0.00 and 0.05 M as shown according to the CVs in Fig. 7. As shown, although the ionic strength of the electrolyte was high enough during setting the pH higher than ~13, but K^+ had enhancing effect on the sensitivity of the anodic peak current. Concentrations above 0.05 M KCl made a two-phase solution and precipitation. Therefore optimum concentration of KCl was estimated to 0.05 M.

3.5. Characterization of conjugated Salen-based polymer

Fig. 8.A shows the SEM image of the conjugated thin film. Based on the images, the thickness of the film was estimated to be 91±1 nm. Consequently, besides the green nature of water, this effect was considered as another advantageous of the use of water as a fraction of electrolyte. Fig. 8.B shows the FT-IR spectra of the synthesized conjugated Salen-based polymer. However the same behavior was observed during evaluation of the FT-IR spectra of the synthesized Salen-based polymers at two reported scan rates, but observation of an absorption peak at frequency of ~1385 cm^{-1} pointed to the C=C bond of the benzene cycle [24], whereas formation of aliphatic C=C bond was evidenced according to the absorption peak positioned at ~1442 cm^{-1}, which were in good agreement with the vibrational frequencies estimated for the C=C based on Ref. [24].

Fig. 8.C shows the XPS spectra of free Salen and the electro-synthesized conjugated Salen-based polymer. Based on the XPS spectra of Salen, the sharp peak positioned at 284.8 eV was attributed to the C_{1s} of the C-C bond. Whereas the peak positioned to the 281.2 eV was related to the C_{1s} of the C=C bond. In addition, the C_{1s} of the C-N bond was positioned at ~288.3 eV. As clearly shown according to the XPS spectra of the synthesized conjugated Salen-based polymer, the peak related to the C-C bond was completely disappeared. Whereas the peak related to the C=C bond was majorly enhanced. In addition, major decrease was observed in the C-N bond that pointed to the formation of conjugated polymer that acted like a novel molecular wire through the electrochemical process.

3.6. Hydrophilicity of conjugated Salen-based polymer

As explained in detail, the formation of C=C bond in the Salen-based polymer led to have conjugated polymer that behaves as molecular wire. The schematic of the reactions during the formation of conjugated polymer has been shown in the Scheme. 2. In this study, UV-Vis. Spectroscopy was adopted to estimate the ratio of $Metal^+$/Salen during formation of the complex.

According to the results, the ratio of K^+/Salen during formation of coordination compound between K^+ and Salen monomer was estimated to be 5.3: 1. Also the same results were estimated during analysis of other alkali meters such as Na^+, K^+ and Li^+. This result pointed to the great capacity of the Salen-based polymer for binding with the alkali species. Therefore, high hydrophobicity was expected for the conjugated Salen-based polymer during the electro-synthesis process. All these results clearly revealed the capability of the fabricated Salen-based polymer for playing role as suitable optical humidity sensor.

3.7. Figures of merit

The trace of the Salen-based optical sensor ranging from 0.0 to 93.0 % RH has been shown in Fig. 9. The same behavior was observed during reversing the humidity trend. Also Fig. 10 shows the linearity of the blue component vs. different %RH values. The results showed good linearity for the blue component (correlation coefficient, R^2,=0.9943) from 5 to ~80% RH. The rate of the change in the humidity of the chamber was controlled for having enough time to stabilize the response of the sensor during sweeping the humidity. Based on comparison to the reference probe, 90% of maximum response time (t_{90} of reference sensor: ~8 s), the response time of the fabricated RH sensor was estimated to be 9.5 s. Also the recovery time of the sensor based on 90% of minimum response (t_{90}) was estimated to be below 10 s. Short rise time (~9.5 s) was also estimated for the fabricated optical humidity sensor. The hysteresis during rapid and alternative contacting the optical; RH sensor to 25 and 60 % RH, during at least 4 times was shown in Fig. 11. In this test the white laser was only used for removing the memory effect during each analysis. At this condition the temperature of the electrode surface was estimated to around 50 ^oC during maximum 60 s time intervals as the recovery time.

As was shown in Fig. 12, the results were compared with those related to the Ref. RH sensor. Minimum difference (less than ~ 2%) was observed between these two RH sensors that revealed the acceptable behavior of the introduced RH sensor during sensing %RH at different

https://dx.doi.org/10.22161/ijaers.4.4.41 *ISSN: 2349-6495(P) | 2456-1908(O)*

environments. The reproducibility of fabricated humidity sensor is also shown in Fig. 12 at ~20 and ~30 % RH, revealing relative standard deviation (RSD, repeatability) of 3.6 % (n=3) for fabricated optical sensor. Also the RSD% (reproducibility) during analysis of ~25 %RH during at least 4 replicate analyses was estimated to be ~4.0, revealing the acceptable reproducibility of the sensor for RH sensing purposes.

About this optical RH sensor, the stability was also evaluated. Linear stability was observed for the fabricated sensor during providing reverse changes between %RH and temperature ranging between 5.0 – 85% for RH and 15 – 50 ^{o}C for the temperature. At a fixed humidity (%RH=~25%), there were no interferences by increasing the temperature up to 50 ^{o}C. In this study, detection limit was defined as three folds of the standard deviation of blank (dry air) to the calibration sensitivity. More improved detection limit was evaluated for the conjugated Salen-based polymer.

3.8. Interferences

The interference of different gases was investigated at room temperature. For this purpose, the humidity sensor was placed in the chamber and high enough value (such as 1000 parts per million) of foreign gases such as CO, CO_2, NOx, CH_4, Ar, He, and volatile organic compounds (VOCs) as well as vapor of Acids Such as HCl were individually introduced to the cell in the 30.0±0.5% RH as standard RH solution. The results are shown in Fig. 13. No noticeable change in blue component clearly revealed the specificity of the fabricated sensor for reliable humidity sensing purpose. The RH behavior of the fabricated RH sensor has also correlated to the number of Salen layers grown on the surface of GC electrode via different successive (repetitive) CV mode up to ~ 20 sequential CV scans. Based on the results, the smoothest surface as well as maximum sensitivity (optical color changes) was observed only for the 10^{th} layer. Therefore this layer was selected as optimum polymer layer.

Based on the results, acceptable sensitivity (color changes and softness) was observed during coating only 10 sequential polymeric layers of the Salen-based polymer. Therefore it was suggested to select this replicate layers during the fabrication of the RH sensor using the recommended procedure.

3.9. Proposed behavior

Based on the results, the probable behavior of the RH behavior of the fabricated sensor was attributed to the filtration properties of conjugated Salen-based polymer. The evidences related to this claim are summarized as follows:

- The optical behavior of the sensor was function of some optical factors such as intensity of the light source as well as the radiation and reflection angles and the alignment of the light during the optical detections. Therefore the electro-synthesized Salen-based polymer seemed to be considered as "*Hydrochromic Reflective Filter*".
- The RH behavior of this sensor was strongly dependent to the smoothness of the surface on which the conjugated Salen-based polymer was grown by the electro-synthesis technique. To approve this effect, the RH responses of the sensor was compared to the graphite (i.d.: 0.2 cm) support under the similar condition. Based on the optical observation, the smooth behavior of the electrode support (GC electrode) was majorly effective on the sensitivity and homogeneity color of the sensor for RH detection. This result was considered as an important evidence for playing role as optical filter.
- The filtration property of the introduced polymer was also evidenced via introducing different %RH environments with gradient of ~5 %RH per second. As shown the color of the polymer was sequentially changed from orange color to violet color.

These results revealed the filtration behavior of the sensor during %RH sensing purposes. However this process could be approved via formation of some humidity perturbations simply by exhaling for several seconds. As clearly shown the filtration properties of the sensor were evidenced during introduction of different %RH values. Probable behavior of the color changing by absorbing the humidity on synthesized polymer could be due to the reflective index shift by change in polymer volume.

IV. CONCLUSIONS

A simple and low cost method has been introduced for fabrication of an optical humidity sensor using conjugated Salen-based polymer. The behavior of each humidity sensor in presence of humidity was studied. It can be concluded that, fabricated humidity sensor had acceptable detection limit (0.17 %), saturated limit (>80 % RH), the least relative standard deviation (RSD=3.0%), short rise time (~9.5 s) also the good enough linearity (R= 0.9971), compared to the RH sensors previously reported in the literature (Table 1). This type of conjugated polymer was adopted as an optical RH sensor. However this sensor partially suffered

https://dx.doi.org/10.22161/ijaers.4.4.41 *ISSN: 2349-6495(P) | 2456-1908(O)*

form a little hysteresis (maximum ~7.5% RH). All in all, the results prove the capability of all studied samples particularly the Salen-based sensor as humidity sensor.

ACKNOWLEDGEMENT

The authors wish to acknowledge the support of this work to Shiraz University Research Council for kindly supporting this work.

REFERENCES

[1] Y. Zhang, K. Yu, R. Xu, D. Jiang, L. Luo, Z. Zhu, Quartz crystal microbalance coated with carbon nanotube films used as humidity sensor, Sens. Actuat. A: Phys. 120 (2005) 142-146.

[2] F. Sattarzadeh, M.M. Doroodmand, M.H. Sheikhi, A. Zarifkar, Fabrication of a Humidity Sensor Based on Chemical Vapor Deposition-Synthesized Single-Walled Carbon Nanotubes, Sci. Adv. Mater. 5 (2013) 557-565.

[3] Z. Chen, C. Lu, Humidity sensors: a review of materials and mechanisms, Sens. Lett. 3 (2005) 274-295.

[4] P.R. Somani, A.K. Viswanath, R. Aiyer, S. Radhakrishnan, Charge transfer complex-forming dyes incorporated in solid polymer electrolyte for optical humidity sensing, Sens. Actuat. B: Chem. 80 (2001) 141-148.

[5] K. Zheng, Y. Zhou, L. Gu, X. Mo, G.R. Patzke, G. Chen, Humidity sensors based on Aurivillius type Bi 2 MO 6 (M= W, Mo) oxide films, Sens. Actuat. B: Chem. 148 (2010) 240-246.

[6] Y. Sakai, Y. Sadaoka, M. Matsuguchi, Humidity sensors based on polymer thin films, Sens. Actuat. B: Chem. 35 (1996) 85-90.

[7] M. Penza, G. Cassano, Relative humidity sensing by PVA-coated dual resonator SAW oscillator, Sens. Actuat. B: Chem. 68 (2000) 300-306.

[8] X. Wang, O. Larsson, D. Platt, S. Nordlinder, I. Engquist, M. Berggren, X. Crispin, An all-printed wireless humidity sensor label, Sens. Actuat. B: Chem. 166 (2012) 556-561.

[9] S.P. Lee, K.-J. Park, Humidity sensitive field effect transistors, Sens. Actuat. B: Chem. 35 (1996) 80-84.

[10] A. Star, T.R. Han, V. Joshi, J.R. Stetter, Sensing with Nafion Coated Carbon Nanotube Field-Effect Transistors, Electroanalysis 16 (2004) 108-112.

[11] J. Boyle, K. Jones, The effects of CO, water vapor and surface temperature on the conductivity of a SnO2 gas sensor, J.Electron.Mater. 6 (1977) 717-733.

[12] M. Neshkova, R. Petrova, V. Petrov, Piezoelectric quartz crystal humidity sensor using chemically modified nitrated polystyrene as water sorbing coating, Anal. Chim. Acta 332 (1996) 93-103.

[13] L.-X. Sun, T. Okada, Simultaneous determination of the concentration of methanol and relative humidity based on a single Nafion (Ag)-coated quartz crystal microbalance, Anal. Chim. Acta 421 (2000) 83-92.

[14] S. Mintova, T. Bein, Nanosized zeolite films for vapor-sensing applications, Micropor. Mesopor. Mater. 50 (2001) 159-166.

[15] H.-W. Chen, R.-J. Wu, K.-H. Chan, Y.-L. Sun, P.-G. Su, The application of CNT/Nafion composite material to low humidity sensing measurement, Sens. Actuat. B: Chem. 104 (2005) 80-84.

[16] T. Yeo, T. Sun, K. Grattan, Fibre-optic sensor technologies for humidity and moisture measurement, Sens. Actuat. A: Phys. 144 (2008) 280-295.

[17] D. Kumar, R. Sharma, Advances in conductive polymers, Europ. Polymer J. 34 (1998) 1053-1060.

[18] P. Capdevlelle, M. Maumy, Redox and conducting polymers based on salen-type metal units; electrochemical study and some characteristics, New J. Chem. 16 (1992) 697-703.

[19] H. Diehl, C.C. Hach, J.C. Bailar, Bis (N, N'-Disalicylalethylenediamine)-μ-Aquodicobalt (II), Inorganic Synthes. 3 (2007) 196-201.

[20] O. Fatibello-Filho, E.R. Dockal, L.H. Marcolino-Junior, M.F. Teixeira, Electrochemical modified electrodes based on metal-salen complexes, Anal. Lett. 40 (2007) 1825-1852.

[21] P.G. Cozzi, Metal–Salen Schiff base complexes in catalysis: practical aspects, Chem. Soc. Rev. 33 (2004) 410-421.

[22] L. Canali, D.C. Sherrington, Utilisation of homogeneous and supported chiral metal (salen) complexes in asymmetric catalysis, Chem. Soc. Rev. 28 (1999) 85-93.

[23] F. Gao, J. Li, F. Kang, Y. Zhang, X. Wang, F. Ye, J. Yang, Preparation and characterization of a poly [Ni (salen)]/multiwalled carbon nanotube composite by in situ electropolymerization as a capacitive material, Phys. Chem. C 115 (2011) 11822-11829.

[24] G. Socrates, Infrared and Raman Characteristic Group Frequencies: Tables and Charts, John Wiley & Sons, 2004.

[25] A. Sun, Z. Li, T. Wei, Y. Li, P. Cui, Highly sensitive humidity sensor at low humidity based on the

https://dx.doi.org/10.22161/ijaers.4.4.41 *ISSN: 2349-6495(P) | 2456-1908(O)*

quaternized polypyrrole composite film, Sens. Actuat. B: Chem. 142 (2009) 197-203.

[26] P.-G. Su, C.-P. Wang, Highly sensitive humidity sensor at low humidity based on the quaternized polypyrrole composite, Flexible humidity sensor based on TiO2 nanoparticles-polypyrrole-poly-[3-(methacrylamino)propyl] trimethyl ammonium chloride composite materials, Sens. Actuat. B: Chem. 129 (2008) 538-543.

[27] Y. Li, Y. Chen, C. Zhang, T. Xue, M. Yang, A humidity sensor based on interpenetrating polymer network prepared from poly(dimethylaminoethyl methacrylate) and poly(glycidyl methacrylate), Sens. Actuat. B: Chem. 125 (2007) 131-137.

[28] P.-G. Su, C.-S. Wang, Novel flexible resistive-type humidity sensor, Sens. Actuat. B: Chem. 123 (2007) 1071-1076.

[29] P.-G. Su, C.-L. Uen, In situ copolymerization of copolymer of methyl methacrylate and [3-(methacrylamino)propyl] trimethyl ammonium chloride on an alumina substrate for humidity sensing, Sens. Actuat. B: Chem. 107 (2005) 317-322.

[30] P.-G. Su, L.-N. Huang, Humidity sensors based on TiO2 nanoparticles/polypyrrole composite thin films, Sens. Actuat. B: Chem. 123 (2007) 501-507.

[31] X. Lv, Y. Li, L. Hong, D. Luo and M. Yang, A highly water-resistive humidity sensor based on silicon-containing polyelectrolytes prepared by one-pot method, Sens. Actuat. B: Chem. 124 (2007) 347-351.

[32] R. Sundaram, Comparative study on micromorphology and humidity sensitive properties of thick film and disc humidity sensors based on semiconducting SnWO4–SnO2 composites, Sens. Actuat. B: Chem. 124 (2007) 429-436.

[33] C.-L. Dai, M.-C. Liu, F.-S. Chen, C.-C. Wu,M.-W. Chang, A nanowire WO3 humidity sensor integrated with micro-heater and inverting amplifier circuit on chip manufactured using CMOS-MEMS technique, Sens. Actuat. B: Chem. 123 (2007) 896-901.

LEGEND TO THE FIGURES

Fig. 1. Schematic of the designed apparatus for humidity sensing process.

Fig. 2. CVs related to the electro-synthesis of conjugated Salen-based polymer using A) Salen monomer (0.04 M) in acetone as solvent and B) different solvents at 0.04 M Salen, pH >13, 0.04 M KCl and 100 mVs^{-1} scan rate.

Fig. 3. Cyclic voltammetry showing the CVs of Salen (0.04 M) during using different ratios of acetone: water as solvent at pH>13, 0.04 KCl and 100 mVs^{-1} scan rate.

Fig. 4. Cyclic voltammetry showing electro-synthesis using Salen (0.04 M) at 100 mV s^{-1} scan rate and at different pH values using different concentrations of KOH and HCl.

Fig. 5. Cyclic voltammetry showing the effect of different cationic species (0.20 M) during the electro-synthesis of Salen-based polymer at 100 mVs^{-1} scan rate and pH >13.

Fig. 6. Photographic image of electrosynthesized Salen-based polymer on the surface of GC electrode during using A) K^+ and B) Na^+ (0.04 M) at ~40% humidity.

Fig. 7. Cyclic voltammetry showing the effect of different concentrations of K^+ on the electro-synthesis of Salen-based polymer at pH >13 and 100 mVs^{-1} scan rate.

Fig. 8. Characterization of conjugated Salen-based polymer including A) SEM, B) FT-IR spectra and C) XPS spectra.

Fig. 9. Trace of RGB parameter vs. %RH.

Fig. 10. Linearity of blue component vs. different %RH values.

Fig. 11. Diagram representing the hysteresis of the fabricated RH sensor according to blue parameter.

Fig. 12. Reproducibility of fabricated RH sensor during contacting with 20 and 30 % RH.

Fig. 13. Effect of coexisting species on the performance of the Salen-based RH sensor during spiking into a standard %RH (50%).

Schem. 1. Proposed mechanism for the electrosynthesis of the conjugated Salen-based polymer.

Schem. 2. Proposed behavior of the conjugated Salen-based humidity sensor.

BIOGRAPHY OF AUTHORS

Mohammad Mahdi Doroodmand

Department of Chemistry, College of Sciences, Shiraz University, Shiraz 71454, Iran. Accociate proffesor in analytical Cheimsitry. Experience: Analytical chemistry, Instrumentation Design, Synthesis of nanostructures, Bioelectrochemistry. Email address: doroodmand@shirazu.ac.ir, Tel: +098-713-6137152, Fax: +098-713-6460788.

Sina Owji

Department of Chemistry, College of Sciences, Shiraz University, Shiraz 71454, Iran. M.S. in analytical Cheimsitry. Experience: Analytical Chemsitry, Detection and determiantion. Email address: s.owji@yahoo.com, Tel: +098-713-6137153, Fax: +098-713-6460788.

https://dx.doi.org/10.22161/ijaers.4.4.41 *ISSN: 2349-6495(P) | 2456-1908(O)*

Fig. 1

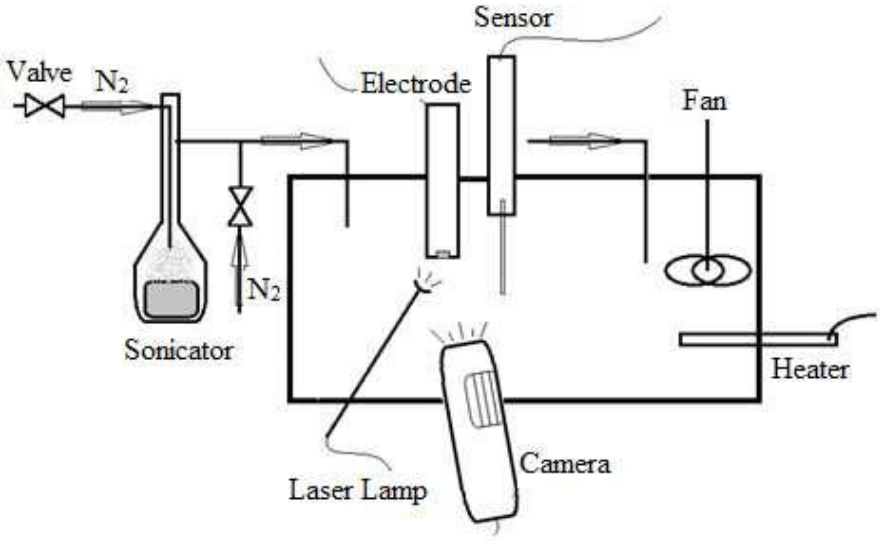

Fig. 2

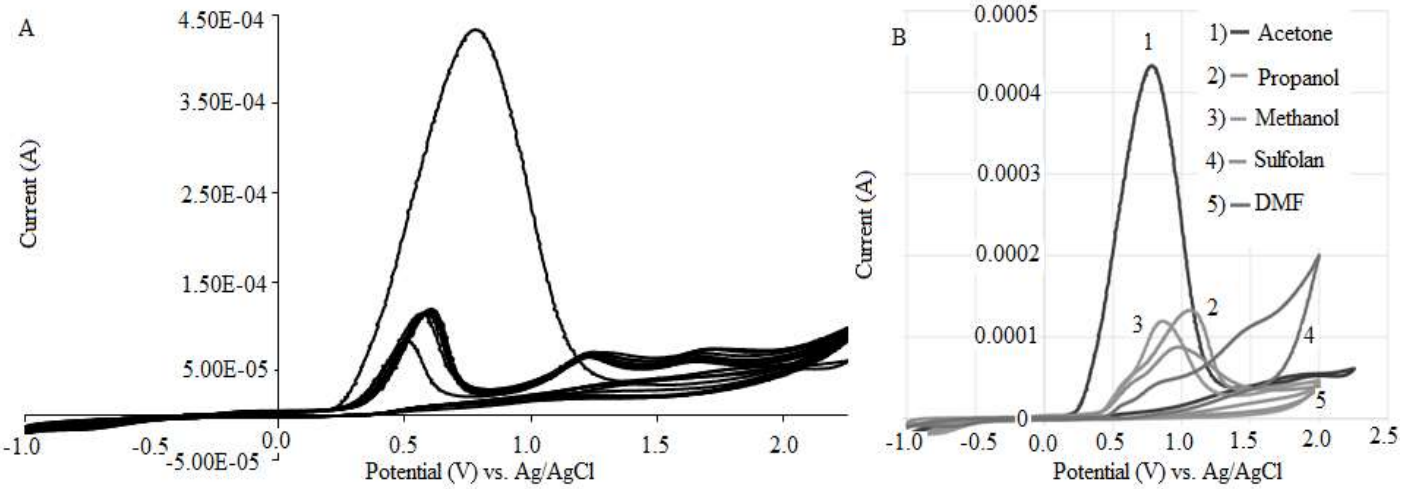

Fig. 3

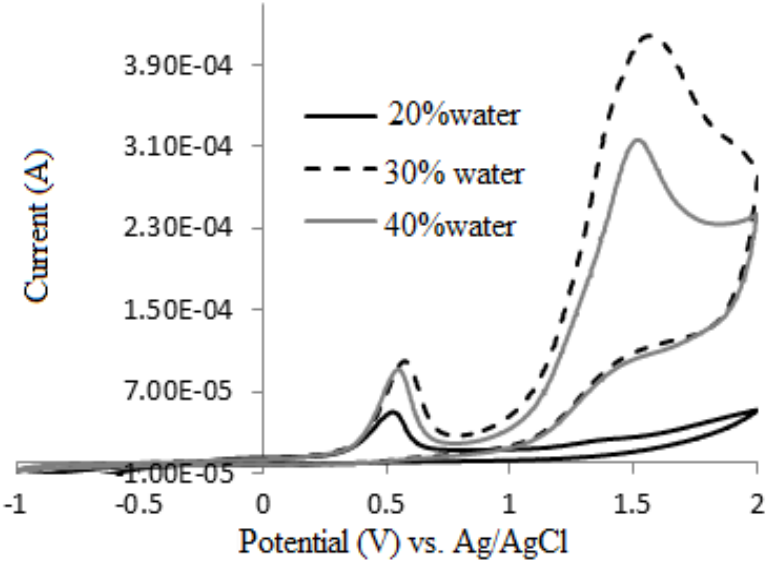

https://dx.doi.org/10.22161/ijaers.4.4.41 *ISSN: 2349-6495(P) | 2456-1908(O)*

Fig. 4

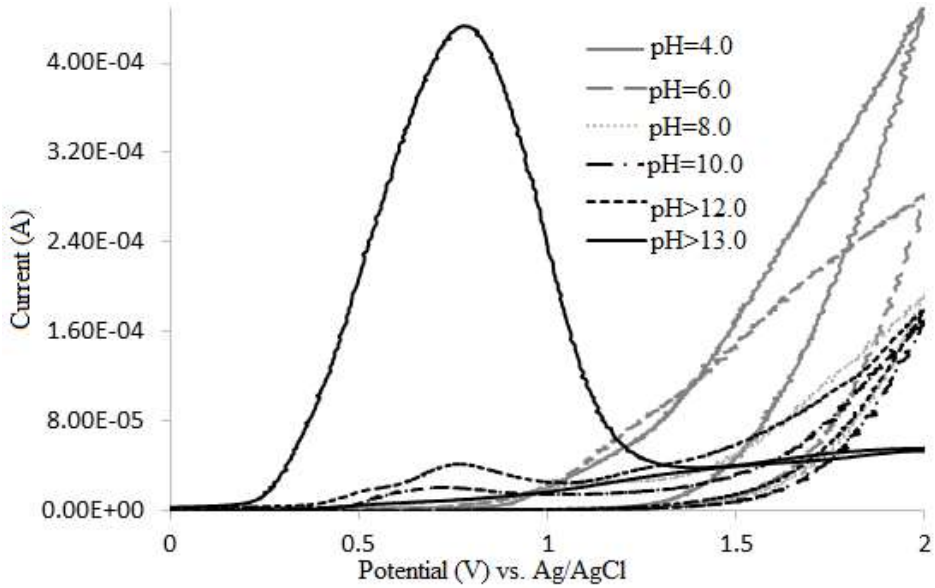

Fig. 5

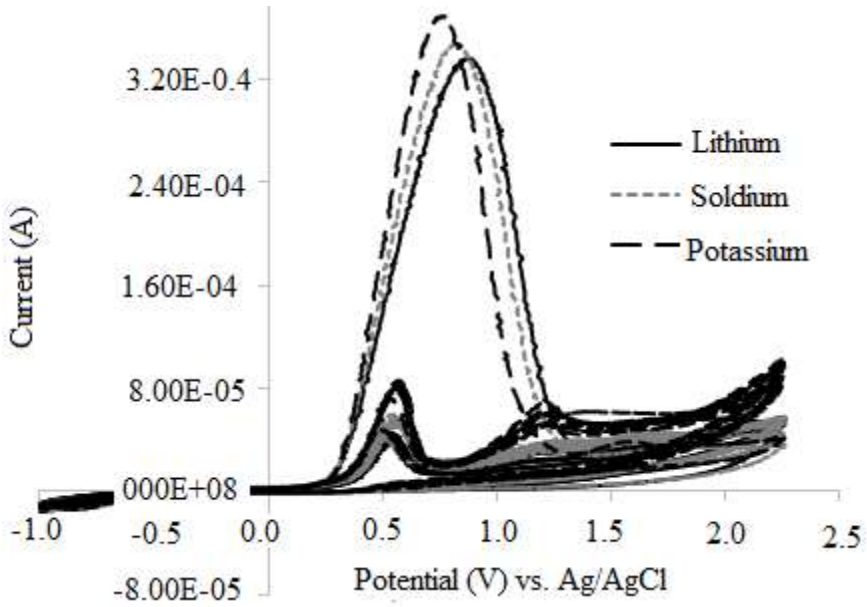

Fig. 6

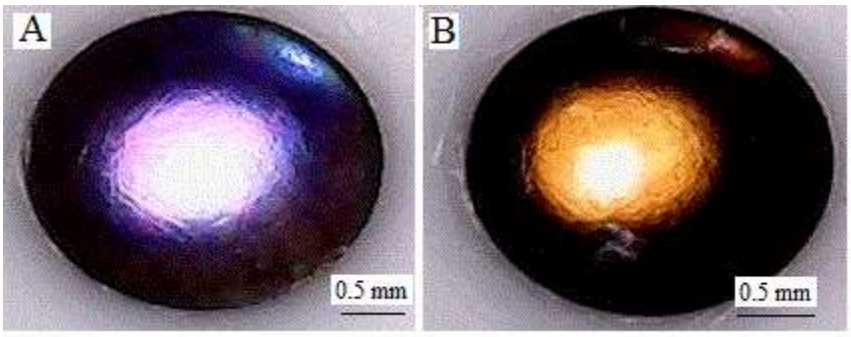

https://dx.doi.org/10.22161/ijaers.4.4.41 *ISSN: 2349-6495(P) | 2456-1908(O)*

Fig. 7

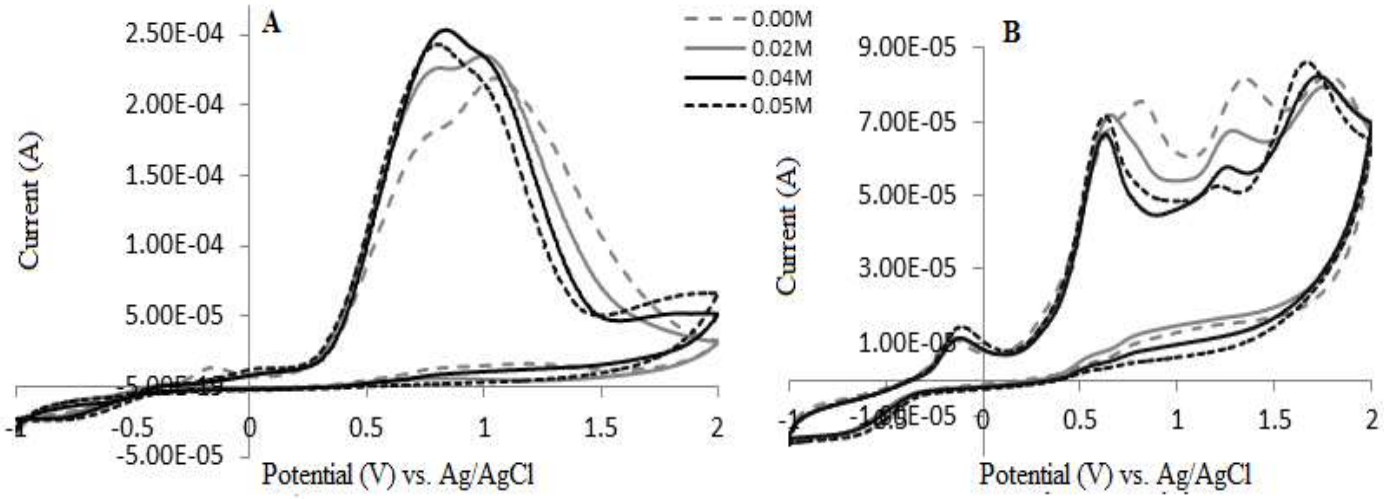

Fig. 8

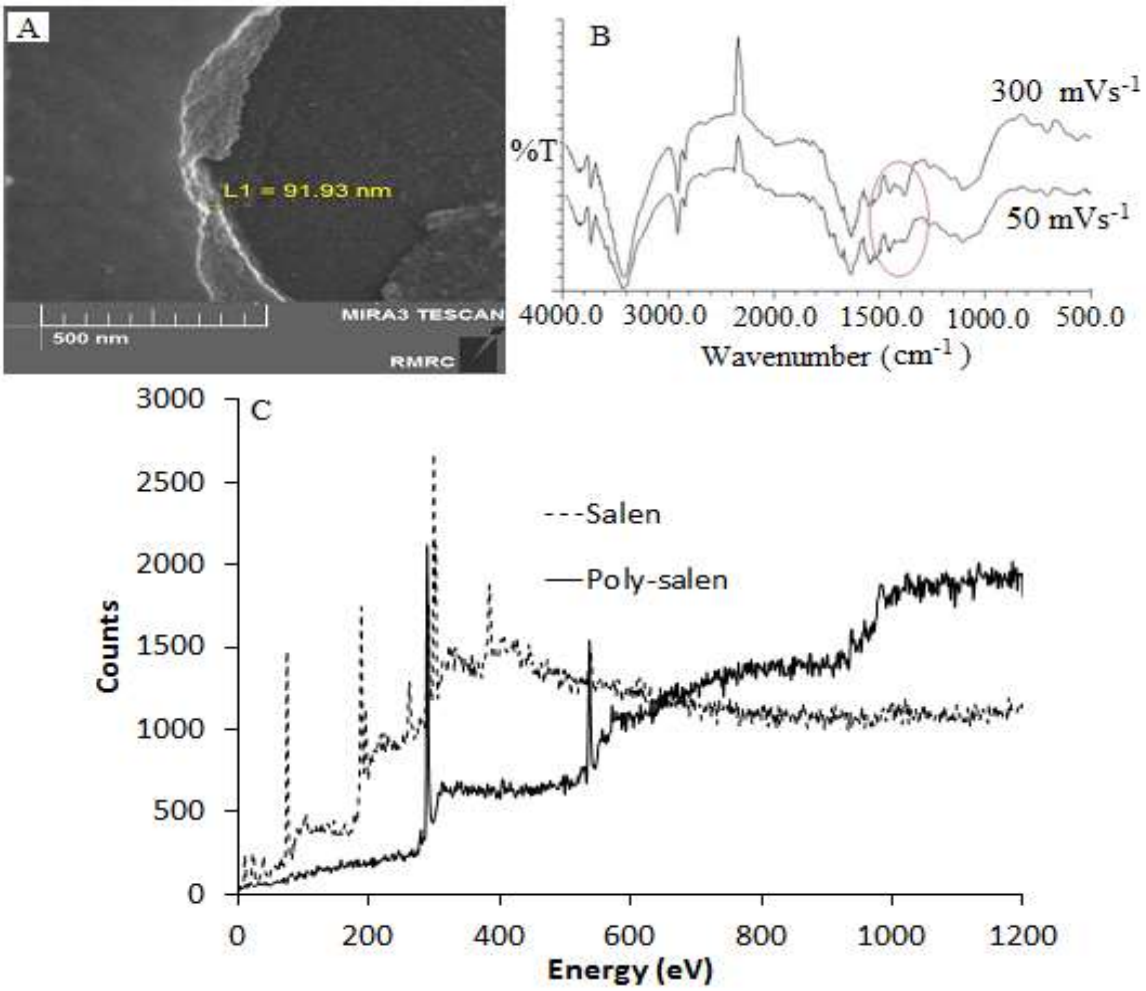

https://dx.doi.org/10.22161/ijaers.4.4.41 *ISSN: 2349-6495(P) | 2456-1908(O)*

Fig. 9

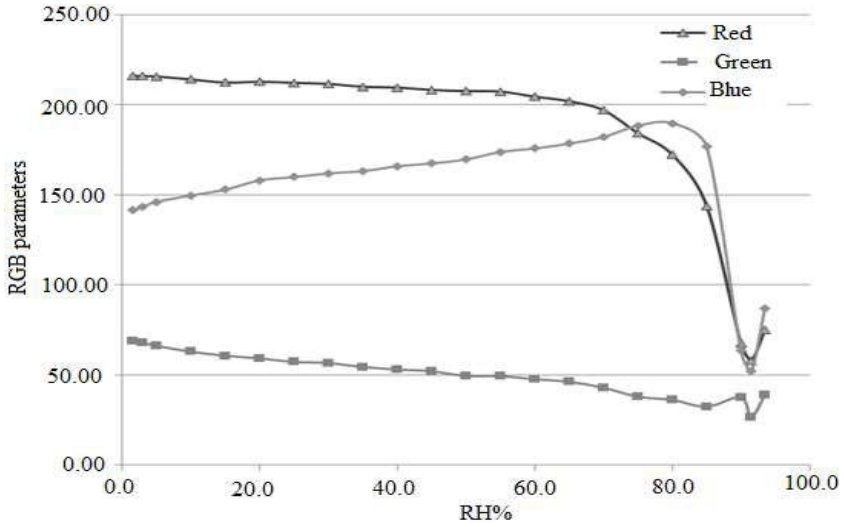

Fig. 10

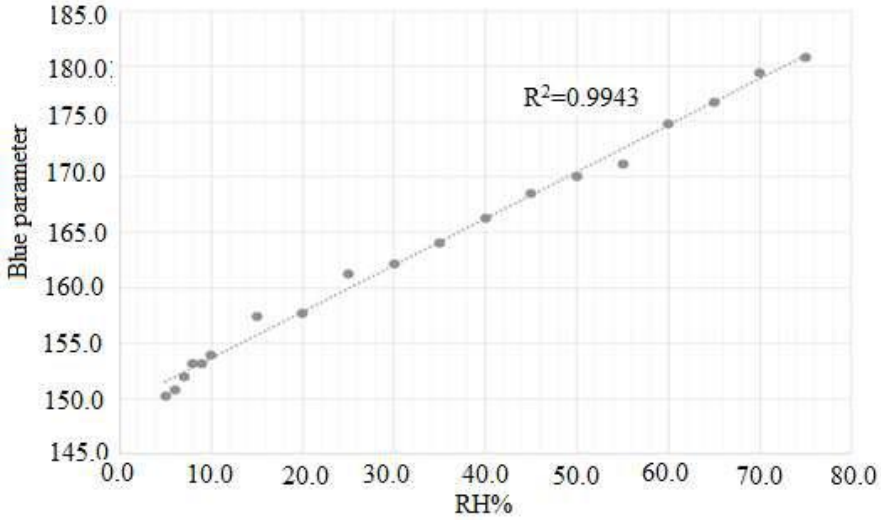

Fig. 11

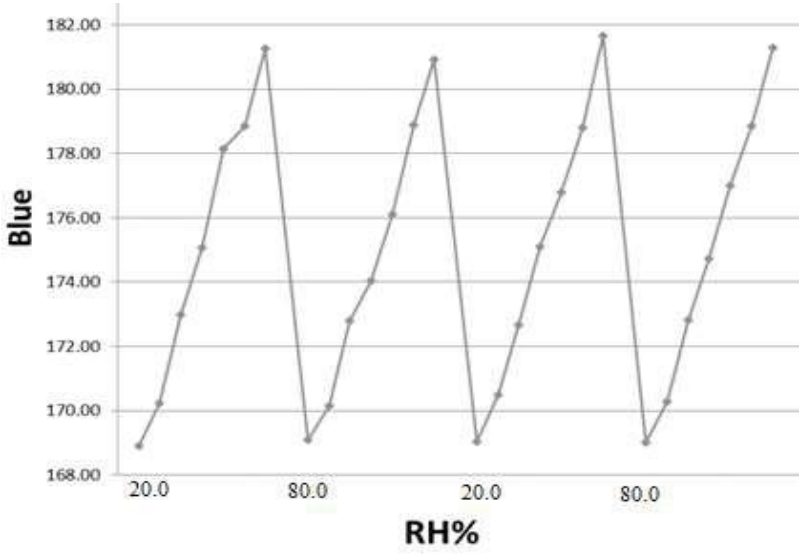

https://dx.doi.org/10.22161/ijaers.4.4.41 *ISSN: 2349-6495(P) | 2456-1908(O)*

Fig. 12

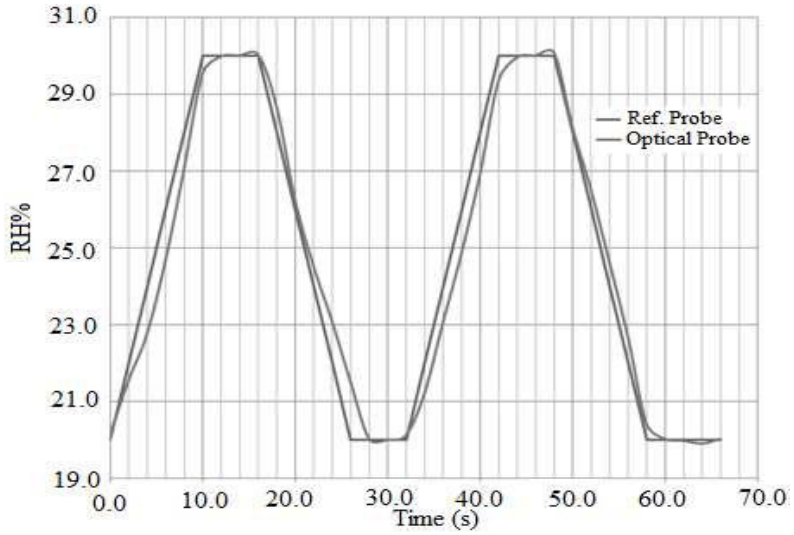

Fig. 13

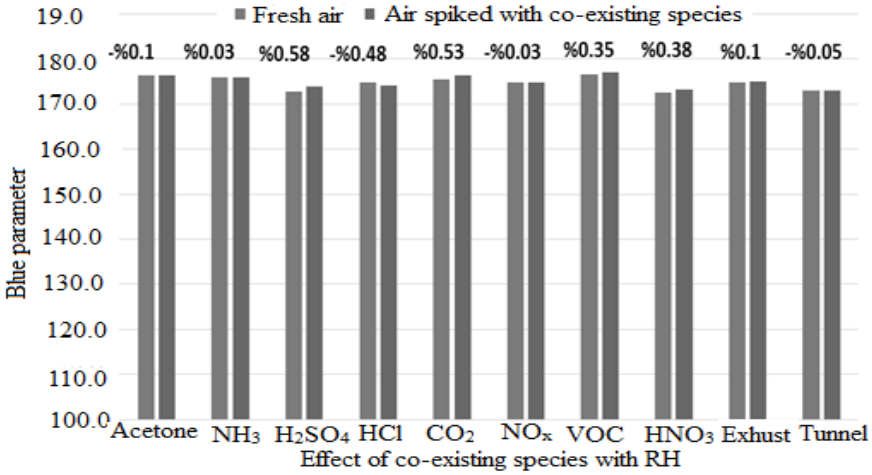

Table.1: Compression between the fabricated sensors with previously reported RH sensors.

Parameter	**Fabricated sensor**	**Previously reported Impedance-based RH sensors**
Linearity (R)	0.9971	0.9916 [25], 0.9972 [26], 0.9894 [27], 0.9351 [28], 0.9315 [29], 0.9491[30]
Standard deviation[1]	3.0	0.1099[25]
Rise time (s)[2]	9.5	41 [25], 30 [26], 45 [28], 30 [29], 40 [30], ~81.5 [31], 300 [32]
Recovery time (s)	10	120 [25], 45 [26], 20 [27], 150 [28], 8 [30], ~226 [31] , 390 [32]
Linear range (%RH)	5-80	11-95 [25], 30–90 [26], 20–97 [27], 10–90 [28, 29], 30–90 [30], 11–97 [31], 5–98 [32], 25–95 [33]
Hysteresis[3] (%RH)	7.5	6.1±0.7 [28], 5.8±0.6[29]
[1.] The standard deviation was obtained by extraction in three replicate analyses.[2.] Time interval needed for 90% of maximum response (t_{90}). [3.] The differences between humidifying and desiccation processes in the range of 20–80%RH.		

https://dx.doi.org/10.22161/ijaers.4.4.41 *ISSN: 2349-6495(P) | 2456-1908(O)*

Graphical Abstract

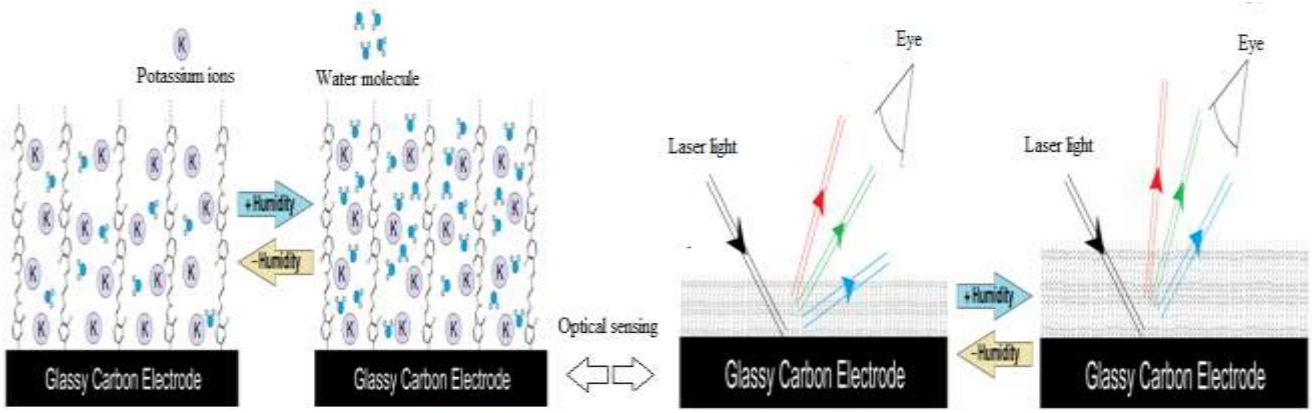

Conjugated Salen-based polymer

Schematic of the humidity sensor

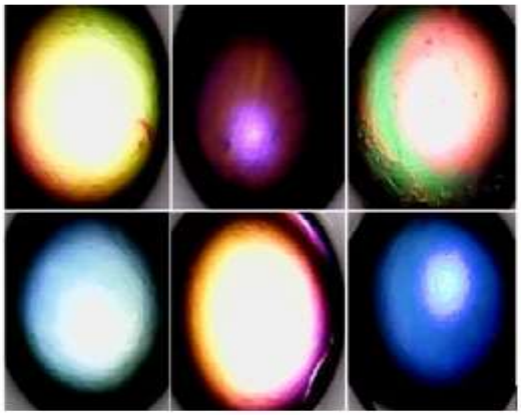

Optical behaviors of the conjugated Salen-based filter during introduction of different humidity environments by the human exhaling. (Colors changes were randomly)